Assessing Scaling in Data Using Wavelets

Brani Vidakovic

GaTech

Workshop in Honor of Professor Pedro A. Morettin
October 19-21, Campinas

Overview

■ The topic as in the talk at Colóquio de Séries Temporais em Homenagem ao 65° Aniversário de Pedro A. Morettin, June 2007 (Campo de Jordao)
However the material different and new.

Overview

■ The topic as in the talk at Colóquio de Séries Temporais em Homenagem ao 65° Aniversário de Pedro A. Morettin, June 2007 (Campo de Jordao)
However the material different and new.

■ Why Scaling in Data is Important?

Overview

■ The topic as in the talk at Colóquio de Séries Temporais em Homenagem ao 65° Aniversário de Pedro A. Morettin, June 2007 (Campo de Jordao)
However the material different and new.

■ Why Scaling in Data is Important?

■ Measures of Scaling – Traditional and Wavelet Based

Overview

■ The topic as in the talk at Colóquio de Séries Temporais em Homenagem ao 65° Aniversário de Pedro A. Morettin, June 2007 (Campo de Jordao)
However the material different and new.

■ Why Scaling in Data is Important?

■ Measures of Scaling – Traditional and Wavelet Based

■ Some New Results: Wavelet Transforms of Images, Robust Measures of Scaling (with thanks to graduate students and two recent visiting scholars).

“Ubiquitous” – The Epithet of Scaling

Atmospheric Turbulence

Frontal component of wind velocity (56Hz) measured at Duke Forrest, Durham, NC.

Atmospheric Turbulence

Frontal component of wind velocity (56Hz) measured at Duke Forrest, Durham, NC.

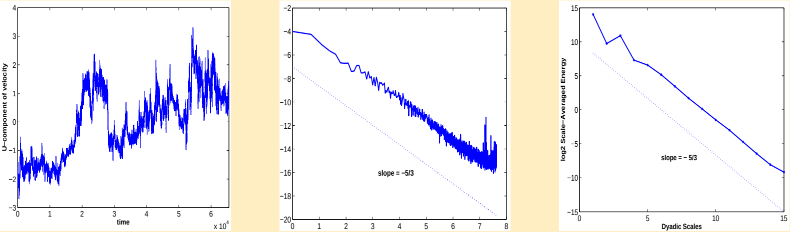

(Left) U Velocity Component; (Middle) Scaling in the Fourier Domain; (Rifgt) Scaling in the Wavelet Domain.
$[5/3 = 2H + 1 \rightarrow H = 1/3]$

Scaling in DNA

A DNA molecule consists of long complementary double helix of purine nucleotides (denoted as A and G) and pyrimidine nucleotides (denoted as C and T). $[A, G \to +1; \;\; C, T \to -1]$

Scaling in DNA

A DNA molecule consists of long complementary double helix of purine nucleotides (denoted as A and G) and pyrimidine nucleotides (denoted as C and T). $[A, G \to +1; \quad C, T \to -1]$

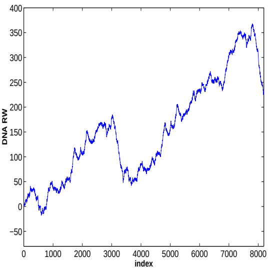

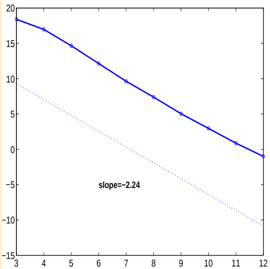

(Left) 8196-long DNA Walk for Spider Monkey, from EMLB Nucleotide Sequence Alignment DNA Database; (Right) Wavelet Scaling With Slope −2.24. $[2.24 = 2H + 1 \to H = 0.62]$

Exchange Rates

Hong Kong Dollar (HKD) versus US Dollar (USD) as reported by the ONADA Company between 24 March 1995 and 1 November 2000.

Exchange Rates

Hong Kong Dollar (HKD) versus US Dollar (USD) as reported by the ONADA Company between 24 March 1995 and 1 November 2000.

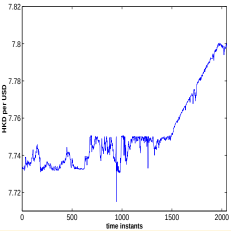

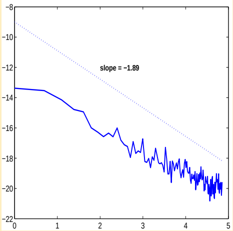

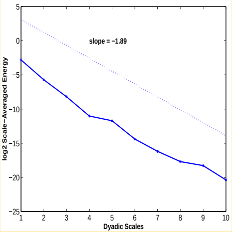

(Left) Exchange Rates HKD per USD; (Right) Scaling behavior in the Fourier domain, and (c) in the wavelet domain.
$[1.89 = 2H + 1 \rightarrow H = 0.455]$

The Stride Interval

Duration of the gait cycle in human walk. Measurements on a healthy subject who walked for 1 hour at normal, slow and fast paces.

The Stride Interval

Duration of the gait cycle in human walk. Measurements on a healthy subject who walked for 1 hour at normal, slow and fast paces.

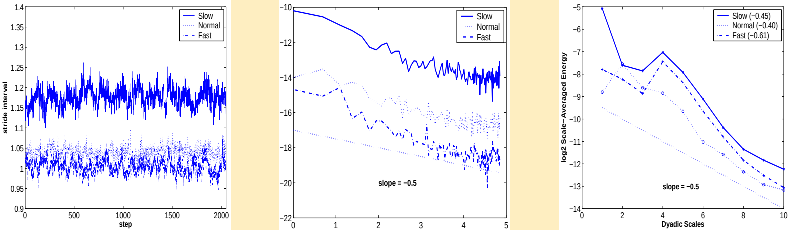

(Left) Gait timing for Slow, Normal and Fast Walk; (Middle) Scaling in the Fourier domain; (Right) In wavelet domain. Slow, normal, and fast stride intervals have slopes of -0.45, -0.4, and -0.61 respectively.

$[\{0.45|0.4|0.61\} = 2H - 1 \rightarrow H = \{0.725|0.7|0.805\}]$

Other Examples

Other Examples

- Various Geophysical High Frequency Measurements (wind velocities, temperatures, chemical and pollutant concentrations, etc.)

Other Examples

- Various Geophysical High Frequency Measurements (wind velocities, temperatures, chemical and pollutant concentrations, etc.)
- Biometric Responses (brain potentials, ocular responses, etc)

Other Examples

- Various Geophysical High Frequency Measurements (wind velocities, temperatures, chemical and pollutant concentrations, etc.)
- Biometric Responses (brain potentials, ocular responses, etc)
- Economic Indices (stock markets, currency exchange, ultra-high frequency data, etc)

Other Examples

- Various Geophysical High Frequency Measurements (wind velocities, temperatures, chemical and pollutant concentrations, etc.)
- Biometric Responses (brain potentials, ocular responses, etc)
- Economic Indices (stock markets, currency exchange, ultra-high frequency data, etc)
- Internet Measurements (internet usage, package sizes, etc)

Other Examples

- Various Geophysical High Frequency Measurements (wind velocities, temperatures, chemical and pollutant concentrations, etc.)
- Biometric Responses (brain potentials, ocular responses, etc)
- Economic Indices (stock markets, currency exchange, ultra-high frequency data, etc)
- Internet Measurements (internet usage, package sizes, etc)
- Industrial Measurements (high speed manufacturing, etc)

Other Examples

- Various Geophysical High Frequency Measurements (wind velocities, temperatures, chemical and pollutant concentrations, etc.)
- Biometric Responses (brain potentials, ocular responses, etc)
- Economic Indices (stock markets, currency exchange, ultra-high frequency data, etc)
- Internet Measurements (internet usage, package sizes, etc)
- Industrial Measurements (high speed manufacturing, etc)
- Astronomy (spatial distributions of stars, astronomical measurements, etc)

Other Examples

- Various Geophysical High Frequency Measurements (wind velocities, temperatures, chemical and pollutant concentrations, etc.)
- Biometric Responses (brain potentials, ocular responses, etc)
- Economic Indices (stock markets, currency exchange, ultra-high frequency data, etc)
- Internet Measurements (internet usage, package sizes, etc)
- Industrial Measurements (high speed manufacturing, etc)
- Astronomy (spatial distributions of stars, astronomical measurements, etc)
- Medicine. Brain and Cancer Research (medical imaging, ultrasound, mass-spectrometry, etc)

Other Examples

- Various Geophysical High Frequency Measurements (wind velocities, temperatures, chemical and pollutant concentrations, etc.)
- Biometric Responses (brain potentials, ocular responses, etc)
- Economic Indices (stock markets, currency exchange, ultra-high frequency data, etc)
- Internet Measurements (internet usage, package sizes, etc)
- Industrial Measurements (high speed manufacturing, etc)
- Astronomy (spatial distributions of stars, astronomical measurements, etc)
- Medicine. Brain and Cancer Research (medical imaging, ultrasound, mass-spectrometry, etc)
- Art (paintings, writings, etc)

Why Should One Care About Scaling?

Because ...

Why Should One Care About Scaling?

Because ...

- If the observations look like "noise" – standard statistical modeling techniques inadequate.

Why Should One Care About Scaling?

Because ...

- If the observations look like "noise" – standard statistical modeling techniques inadequate.
- In denoising applications when there is superposition of two noises, white and colored, scaling helps in filtering.

Why Should One Care About Scaling?

Because ...

- If the observations look like "noise" – standard statistical modeling techniques inadequate.
- In denoising applications when there is superposition of two noises, white and colored, scaling helps in filtering.
- Need to simulate processes that scale (queueing systems, internet, surrogate data in geosciences, wavestrapping, bootstrap tests, etc.)

Why Should One Care About Scaling?

Because ...

- If the observations look like "noise" – standard statistical modeling techniques inadequate.
- In denoising applications when there is superposition of two noises, white and colored, scaling helps in filtering.
- Need to simulate processes that scale (queueing systems, internet, surrogate data in geosciences, wavestrapping, bootstrap tests, etc.)
- Summaries of fractal/multifractal spectra as descriptors/data summaries.

Types of Scaling

Regular Scaling

Types of Scaling

Regular Scaling

- Monofractals, Several Popular Theoretical Models

Types of Scaling

Regular Scaling

- Monofractals, Several Popular Theoretical Models
- Regular: Plot of **Log(AverageEnergy**) versus **Log(Scale)** is a straight line.

Types of Scaling

Regular Scaling

- Monofractals, Several Popular Theoretical Models
- Regular: Plot of **Log(AverageEnergy**) versus **Log(Scale)** is a straight line.
- In Wavelet Terms: Plot of **Log2(LevelwiseMean(Wavelet Coefficients Squared))** versus **Level Number** is a straight line.

Types of Scaling

Regular Scaling

- Monofractals, Several Popular Theoretical Models
- Regular: Plot of **Log(AverageEnergy**) versus **Log(Scale)** is a straight line.
- In Wavelet Terms: Plot of **Log2(LevelwiseMean(Wavelet Coefficients Squared))** versus **Level Number** is a straight line.

Irregular Scaling

Types of Scaling

Regular Scaling

- Monofractals, Several Popular Theoretical Models
- Regular: Plot of **Log(AverageEnergy**) versus **Log(Scale)** is a straight line.
- In Wavelet Terms: Plot of **Log2(LevelwiseMean(Wavelet Coefficients Squared))** versus **Level Number** is a straight line.

Irregular Scaling

- Type I (Local Monofractals, Time- or Space-Dependent Hurst Exponent)

Types of Scaling

Regular Scaling

- Monofractals, Several Popular Theoretical Models
- Regular: Plot of **Log(AverageEnergy**) versus **Log(Scale)** is a straight line.
- In Wavelet Terms: Plot of **Log2(LevelwiseMean(Wavelet Coefficients Squared))** versus **Level Number** is a straight line.

Irregular Scaling

- Type I (Local Monofractals, Time- or Space-Dependent Hurst Exponent)
- Type II (Multifractals, Distribution of Irregularity Indices.

Irregular Scaling: mfBm(H_t)

Multifractional Brownian Motions generated with (a) $H_t = 0.8t + 0.1$; (b) $H_t = 0.1 + 3.2(t - 0.5)^2,\ 0 < t < 1$. H_t is estimated by Local Quadratic Variations of sample paths (Couerjolly, PhD Thesis 2000).

Irregular Scaling: mfBm(H_t)

Multifractional Brownian Motions generated with (a) $H_t = 0.8t + 0.1$; (b) $H_t = 0.1 + 3.2(t - 0.5)^2,\ 0 < t < 1$. H_t is estimated by Local Quadratic Variations of sample paths (Couerjolly, PhD Thesis 2000).

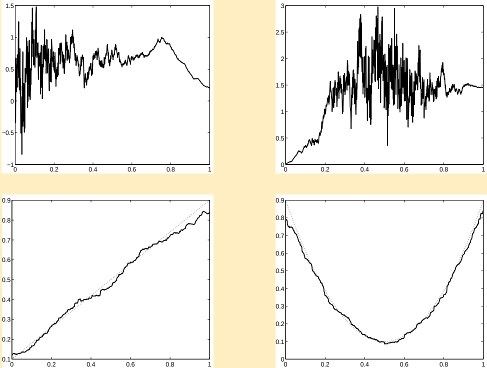

Irregular Scaling: mf spectra

Turbulence (multifractal) and fBm with $H = 1/3$ (monofractal) are indistinguishable wrt the second order properties. Testing for Monoftactality (Sky Lee, PhD Thesis 2010)

Irregular Scaling: mf spectra

Turbulence (multifractal) and fBm with $H = 1/3$ (monofractal) are indistinguishable wrt the second order properties. Testing for Monoftactality (Sky Lee, PhD Thesis 2010)

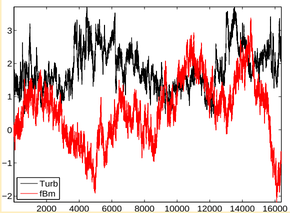

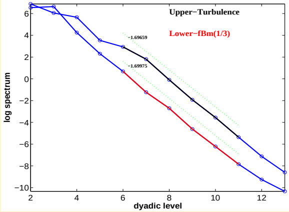

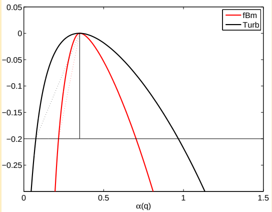

Model

Model

- Random process $X(t),\ t \geq 0$ is self-similar, with self-similarity index H (H-ss) if and only if there exists $H > 0$ such that for any $a > 0$, $X(at) \stackrel{d}{=} a^H X(t)$.

Model

- Random process $X(t),\ t \geq 0$ is self-similar, with self-similarity index H (H-ss) if and only if there exists $H > 0$ such that for any $a > 0$, $X(at) \stackrel{d}{=} a^H X(t)$.
- Standard Brownian Motion $B(t)$ is 1/2-ss since the process $W(t) = 1/\sqrt{a}B(at)$ is standard Brownian motion, as well.

Model

- Random process $X(t),\ t \geq 0$ is self-similar, with self-similarity index H (H-ss) if and only if there exists $H > 0$ such that for any $a > 0$, $X(at) \stackrel{d}{=} a^H X(t)$.
- Standard Brownian Motion $B(t)$ is 1/2-ss since the process $W(t) = 1/\sqrt{a}B(at)$ is standard Brownian motion, as well.
- Let $X(t), t \in R$ be $H - ss$ process. If its increments $X(t+h) - X(t)$ are stationary, $X(t)$ is called $H - sssi$ process.

Model

- Random process $X(t),\ t \geq 0$ is self-similar, with self-similarity index H (H-ss) if and only if there exists $H > 0$ such that for any $a > 0$, $X(at) \overset{d}{=} a^H X(t)$.
- Standard Brownian Motion $B(t)$ is 1/2-ss since the process $W(t) = 1/\sqrt{a}B(at)$ is standard Brownian motion, as well.
- Let $X(t), t \in R$ be $H - ss$ process. If its increments $X(t+h) - X(t)$ are stationary, $X(t)$ is called $H - sssi$ process.
- $fBm(H)$ is a zero mean Gaussian process for which

$$EB_H(t)B_H(s) = \frac{E|B_H(1)|^2}{2}\left[|t|^{2H} + |s|^{2H} - |t-s|^{2H}\right],$$

where $E|B_H(1)|^2 = \frac{\Gamma(2-2H)\cos(\pi H)}{\pi H(1-2H)}$.

Model

- Random process $X(t),\ t \geq 0$ is self-similar, with self-similarity index H (H-ss) if and only if there exists $H > 0$ such that for any $a > 0$, $X(at) \stackrel{d}{=} a^H X(t)$.
- Standard Brownian Motion $B(t)$ is 1/2-ss since the process $W(t) = 1/\sqrt{a}B(at)$ is standard Brownian motion, as well.
- Let $X(t), t \in R$ be $H - ss$ process. If its increments $X(t+h) - X(t)$ are stationary, $X(t)$ is called $H - sssi$ process.
- $fBm(H)$ is a zero mean Gaussian process for which

$$EB_H(t)B_H(s) = \frac{E|B_H(1)|^2}{2}\left[|t|^{2H} + |s|^{2H} - |t-s|^{2H}\right],$$

  where $E|B_H(1)|^2 = \frac{\Gamma(2-2H)\cos(\pi H)}{\pi H(1-2H)}$.
- $fBm(H) \equiv$ **unique** Gaussian $H - sssi$ process.

Fractional Brownian Field (2D-fBm)

Fractional Brownian Field (2D-fBm)

A 2D-fBm, $B_H(\mathbf{t})$, for $\mathbf{t} \in \mathbb{R}^+ \times \mathbb{R}^+$ and $H \in (0,1)$, is a process with stationary zero-mean Gaussian increments,

$$B_H(a\mathbf{t}) \stackrel{d}{=} a^H B_H(\mathbf{t}),$$

$$\mathbb{E}\left[B_H(\mathbf{t})B_H(\mathbf{s})\right] = \frac{\sigma_H^2}{2}\left(\|\mathbf{t}\|^{2H} + \|\mathbf{s}\|^{2H} - \|\mathbf{t}-\mathbf{s}\|^{2H}\right).$$

B. Pesquet-Popescu and J.L. Vehel, 2002

Fractional Brownian Field (2D-fBm)

A 2D-fBm, $B_H(\mathbf{t})$, for $\mathbf{t} \in \mathbb{R}^+ \times \mathbb{R}^+$ and $H \in (0,1)$, is a process with stationary zero-mean Gaussian increments,

$$B_H(a\mathbf{t}) \stackrel{d}{=} a^H B_H(\mathbf{t}),$$

$$\mathbb{E}\left[B_H(\mathbf{t})B_H(\mathbf{s})\right] = \frac{\sigma_H^2}{2}\left(\|\mathbf{t}\|^{2H} + \|\mathbf{s}\|^{2H} - \|\mathbf{t}-\mathbf{s}\|^{2H}\right).$$

B. Pesquet-Popescu and J.L. Vehel, 2002

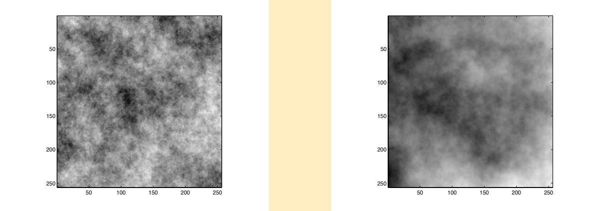

Figure: Fractional Brownian fields for (Left) $H = 1/3$ and (Right) $H = 3/4$.

Estimation of H

Estimation of H

- Methods Based on Contrasting Various Estimators of Variance

Estimation of H

- Methods Based on Contrasting Various Estimators of Variance
- Methods Based on Various Aspects of Fourier Spectra (Whittle, Periodogram, ...)

Estimation of H

- Methods Based on Contrasting Various Estimators of Variance
- Methods Based on Various Aspects of Fourier Spectra (Whittle, Periodogram, ...)
- Methods Based on Zero-Level-Crossings of Paths

Estimation of H

- Methods Based on Contrasting Various Estimators of Variance
- Methods Based on Various Aspects of Fourier Spectra (Whittle, Periodogram, ...)
- Methods Based on Zero-Level-Crossings of Paths
- Methods Based on Quadratic Variations

Estimation of H

- Methods Based on Contrasting Various Estimators of Variance
- Methods Based on Various Aspects of Fourier Spectra (Whittle, Periodogram, ...)
- Methods Based on Zero-Level-Crossings of Paths
- Methods Based on Quadratic Variations
- Methods Based on Convex Rearrangements

Multiscale Paradigm

Estimation of H

- Methods Based on Contrasting Various Estimators of Variance
- Methods Based on Various Aspects of Fourier Spectra (Whittle, Periodogram, ...)
- Methods Based on Zero-Level-Crossings of Paths
- Methods Based on Quadratic Variations
- Methods Based on Convex Rearrangements

Multiscale Paradigm

- Identify a hierarchy of scales in the multiscale decomposition

Estimation of H

- Methods Based on Contrasting Various Estimators of Variance
- Methods Based on Various Aspects of Fourier Spectra (Whittle, Periodogram, ...)
- Methods Based on Zero-Level-Crossings of Paths
- Methods Based on Quadratic Variations
- Methods Based on Convex Rearrangements

Multiscale Paradigm

- Identify a hierarchy of scales in the multiscale decomposition
- Fit the linear propagation of "log-energies" across the scales

Estimation of H

- Methods Based on Contrasting Various Estimators of Variance
- Methods Based on Various Aspects of Fourier Spectra (Whittle, Periodogram, ...)
- Methods Based on Zero-Level-Crossings of Paths
- Methods Based on Quadratic Variations
- Methods Based on Convex Rearrangements

Multiscale Paradigm

- Identify a hierarchy of scales in the multiscale decomposition
- Fit the linear propagation of "log-energies" across the scales
- Transform the slopes of the fits to the regularity indices

Estimation of H

- Methods Based on Contrasting Various Estimators of Variance
- Methods Based on Various Aspects of Fourier Spectra (Whittle, Periodogram, ...)
- Methods Based on Zero-Level-Crossings of Paths
- Methods Based on Quadratic Variations
- Methods Based on Convex Rearrangements

Multiscale Paradigm

- Identify a hierarchy of scales in the multiscale decomposition
- Fit the linear propagation of "log-energies" across the scales
- Transform the slopes of the fits to the regularity indices

- "Waveletize" methods that use filtering (Quadratic Variations, Convex Rearrangements, Lorenzians, ...

In the rest of the talk...

- 2-D Scale Mixing Wavelet Transform
- Estimating H from Scale-Mixing Spectra
- Robust Estimator of H (Theil-Sen-Type Estimator)
- Application: Breast Cancer Diagnostics
- An Approach Based on Convex Rearrangements (If time permits)

1D Wavelet Transform via a Matrix

- Given the wavelet basis (via its filter $\boldsymbol{h}$), form an orthogonal matrix W of size $N \times N$ so that for signal $\boldsymbol{y}$, $\boldsymbol{d} = W \cdot \boldsymbol{y}$.
- Matrix $W = W_J$ is defined iteratively (J is the depth of transform)

$$W_1 = \begin{bmatrix} H_1 \\ G_1 \end{bmatrix}, \quad W_2 = \begin{bmatrix} \begin{bmatrix} H_2 \\ G_2 \end{bmatrix} \cdot H_1 \\ G_1 \end{bmatrix},$$

$$W_3 = \begin{bmatrix} \begin{bmatrix} \begin{bmatrix} H_3 \\ G_3 \end{bmatrix} \cdot H_2 \\ G_2 \end{bmatrix} \cdot H_1 \\ G_1 \end{bmatrix}, \dots$$

1D Wavelet Transform via a Matrix

- Given the wavelet basis (via its filter $\boldsymbol{h}$), form an orthogonal matrix W of size $N \times N$ so that for signal $\boldsymbol{y}$, $\boldsymbol{d} = W \cdot \boldsymbol{y}$.
- Matrix $W = W_J$ is defined iteratively (J is the depth of transform)

$$W_1 = \begin{bmatrix} H_1 \\ G_1 \end{bmatrix}, \quad W_2 = \begin{bmatrix} \begin{bmatrix} H_2 \\ G_2 \end{bmatrix} \cdot H_1 \\ G_1 \end{bmatrix},$$

$$W_3 = \begin{bmatrix} \begin{bmatrix} \begin{bmatrix} H_3 \\ G_3 \end{bmatrix} \cdot H_2 \\ G_2 \end{bmatrix} \cdot H_1 \\ G_1 \end{bmatrix}, \ldots$$

- Given filter $\boldsymbol{h} = (h_0, h_1, \dots)$, H_k a matrix with (i, j)th element

$$h_s, \text{ for } s = (N-1) + (i-1) - 2(j-1) \text{ modulo } 2^{J-k+1}.$$

- Matrix G_k formed as H_k but with the QM filter $\boldsymbol{g}$.

Scale-mixing Transform

- Let A be an image of dyadic size, $2^n \times 2^n$. Form a wavelet matrix W of the same size.
- The object WA' represents a matrix in which columns are wavelet transformed rows of A. If the same is repeated with the rows of WA' the result is

  $$B = W(WA')' = WAW'.$$

  Matrix B is called scale mixing wavelet transform of A.
- The inverse is straightforward: $A = W'BW$.
- "Energy" preserved: $E = \text{trace}(AA') = \text{trace}(BB')$.
- Easy to generalize to different wavelets (different left- and right-hand side matrices W_1, W_2) and to rectangular sizes of A.

Tessellations by 2D WT: Traditional, Scale-mixing, and a Mix

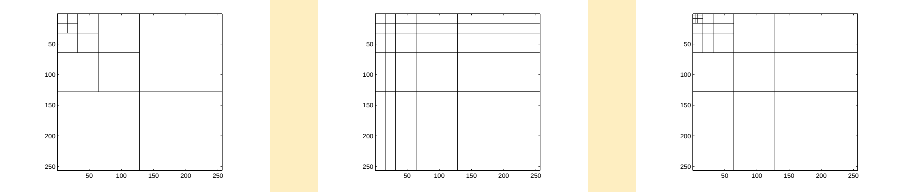

Figure: Tiling images by (Left) Traditional 2-D Wavelet Transform; (Middle) Scale-mixing Wavelet Transform; and (Right) Generalized 2-D Wavelet Transform

Tessellations by 2D WT: Traditional, Scale-mixing, and a Mix

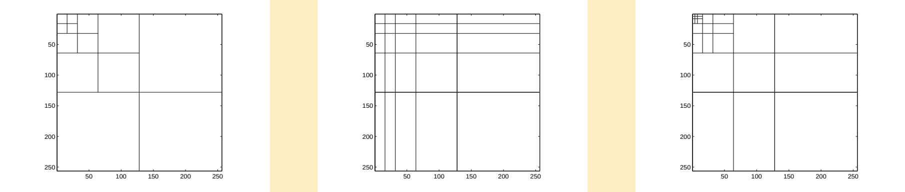

Figure: Tiling images by (Left) Traditional 2-D Wavelet Transform; (Middle) Scale-mixing Wavelet Transform; and (Right) Generalized 2-D Wavelet Transform

• Any hierarchy of self-similar multiresolution subspaces leads to a spectra.

• For traditional wavelet transforms three spectra usually defined as: horizontal, vertical, and diagonal (Nicolis et al, 2011).

Hierarchies in Scale-mixing 2-D WT

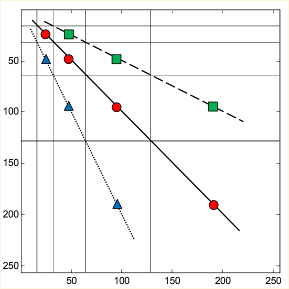

Figure: Hierarchies $(j, j+s)$ for $s = 0 \pm 1$

• Given an isotropic random field, all hierarchies $(j, j+s)$, s fixed lead to the same power law.

• If one component is fixed, (j_0, j) or (j_0, j) the power law exist, but depends on size matrix A and j_0. Empirically if j_0 is the finest level of detail, slope in the spectra $\approx -H$.

Result (Ramírez Cobo et al., 2011)

If $d_{(j,j+s)}$ $(= d_{(j,j+s;k_1,k_2)},\; j = j_0, \ldots, j_1;\; s$ fixed), is a wavelet coefficient in a scale-mixing decomposition of 2D fBm

$$\log_2 \mathbb{E}\left[d^2_{(j,j+s)}\right] = -(2H+2)j + C_{\psi,s,H}$$

Result (Ramírez Cobo et al., 2011)

If $d_{(j,j+s)}$ ($= d_{(j,j+s;k_1,k_2)},\ j = j_0, \ldots, j_1;\ s$ fixed), is a wavelet coefficient in a scale-mixing decomposition of 2D fBm

$$\log_2 \mathbb{E}\left[d^2_{(j,j+s)}\right] = -(2H+2)j + C_{\psi,s,H}$$

Hurst exponent can be estimated from the regression slope.

Fitting the Linear Regression

- Average d^2 over the level, take the logs (mean-first) [Abry and collaborators] $(j, \log_2 \overline{d_j^2})$
- Take the logs of d^2, then average over the level (log-first) [Taqqu and collaborators] $(j, \overline{\log_2 d_j^2})$
- Average a few d^2, take the logs, take average (mean-log-mean) [Soltani and collaborators] $(j, \overline{\log_2 \overline{d_j^2}})$

Estimating Slope: Approaches

- OLS – wrong methodology – but works OK.
- Weighted LS (Abry & Veitch, 1999)
  $y_j = \log \overline{d_j^2} + 1/(n_j \log 2), \quad n_j$ is the number of ds in level j.
  $\widehat{sl} = \sum_j w_j y_j$, where $w_j = (S_0 j - S_1)/(S_0 S_2 - S_1^2)$
  $S_k = \sum_j j^k/\sigma_j^2,\ k = 0, 1, 2$ and $\sigma_j^2 = 2/(n_j \log^2 2)$

Estimating Slope: Approaches

- OLS – wrong methodology – but works OK.
- Weighted LS (Abry & Veitch, 1999)
  $y_j = \log \overline{d_j^2} + 1/(n_j \log 2), \quad n_j$ is the number of ds in level j.
  $\widehat{sl} = \sum_j w_j y_j$, where $w_j = (S_0 j - S_1)/(S_0 S_2 - S_1^2)$
  $S_k = \sum_j j^k/\sigma_j^2,\ k = 0, 1, 2$ and $\sigma_j^2 = 2/(n_j \log^2 2)$

Theil-Sen-Type Estimator (Hamilton et al, 2011)

- Find all pairwise slopes $s_{ij} = (\log \overline{d_j^2} - \log \overline{d_i^2})/(j - i)$ generated by two points $(i, \log \overline{d_i^2})$ and $(j, \log \overline{d_j^2})$, $j_{min} < i < j < j_{max}$.
- Estimate the slope as a weighted average of pairwise slopes corrected for the bias.
- What are optimal weights?

Derivation of TS-Type Estimator

- Start with m-D fBm $B_H(\omega, \mathbf{t})$ and transform it to the wavelet domain. Consider the main diagonal hierarchy ($s = 0$), a multiresolution ladder indexed by j.

$$d_j \sim \mathcal{N}(0, 2^{-(2H+m)j}\sigma^2).$$

- The coefficients d_j within the level j are (typically) considered approximately independent (Flandrin, 1992). At level j there are 2^{mj} coefficients. Thus,

$$\overline{d_j^2} \overset{d}{=} 2^{-(2H+2m)j}\sigma^2\chi^2_{2^{mj}}.$$

- Expectation and variance of average level-energies

$$\mathbb{E}\overline{d_j^2} = 2^{-(2H+m)j}\sigma^2, \qquad \mathbb{V}\mathbf{ar}\,\overline{d_j^2} = 2^{-4Hj-3mj+1}\sigma^4$$

$$\mathbb{E}\varphi(X) \approx \varphi(\mathbb{E}X) + \frac{1}{2}\varphi''(\mathbb{E}X) \cdot \mathbb{V}\mathbf{ar}\, X$$
$$\mathbb{V}\mathbf{ar}\, \varphi(X) \approx (\varphi'(\mathbb{E}X))^2 \mathbb{V}\mathbf{ar}\, X.$$

When φ is logarithm for base 2, then

$$\mathbb{E} \log_2 \overline{d_j^2} = -(2H + m)j - \frac{1}{2^{mj} \log 2} + \log_2 \sigma^2.$$

$$\mathbb{E}\varphi(X) \approx \varphi(\mathbb{E}X) + \frac{1}{2}\varphi''(\mathbb{E}X) \cdot \mathbb{V}\mathbf{ar}\, X$$
$$\mathbb{V}\mathbf{ar}\, \varphi(X) \approx (\varphi'(\mathbb{E}X))^2 \mathbb{V}\mathbf{ar}\, X.$$

When φ is logarithm for base 2, then

$$\mathbb{E} \log_2 \overline{d_j^2} = -(2H + m)j - \frac{1}{2^{mj} \log 2} + \log_2 \sigma^2.$$

$$\mathbb{V}\mathbf{ar}\ \log_2 \overline{d_j^2} = \frac{2}{2^{mj} (\log 2)^2}.$$

- Variance of the pairwise slope s_{ij} is

$$\mathbb{V}\mathbf{ar}\, s_{ij} = \mathbb{V}\mathbf{ar}\left(\frac{\log_2 \overline{d_j^2} - \log_2 \overline{d_i^2}}{j-i}\right) = \frac{2}{(\log 2)^2} \cdot \frac{1/2^{mj} + 1/2^{mi}}{(j-i)^2}.$$

- Take weights w_{ij} inverse-proportional to the variance of s_{ij},

$$w_{ij} \propto (i-j)^2 \times HA(2^{mi}, 2^{mj}), \quad \sum_{i<j} w_{ij} = 1,$$

where HA is the harmonic average of level sizes.

$$s_{ij}^* = s_{ij} + \frac{1}{(j-i)\log 2}\left(\frac{1}{2^{mj}} - \frac{1}{2^{mi}}\right)$$

Theil-Sen-Type Estimator: Slope estimated by $\sum_{i,j} w_{ij} s_{ij}^*$

Data: Mammogram Images

- Digitized mammograms from University South Florida Digital Database for Screening Mammography (DDSM)
- Gold standard was biopsy
- 105 normal and 72 cancer craniocaudal (CC) images
- A subimage of size 1024×1024 taken from each image

Data: Mammogram Images

- Digitized mammograms from University South Florida Digital Database for Screening Mammography (DDSM)
- Gold standard was biopsy
- 105 normal and 72 cancer craniocaudal (CC) images
- A subimage of size 1024×1024 taken from each image

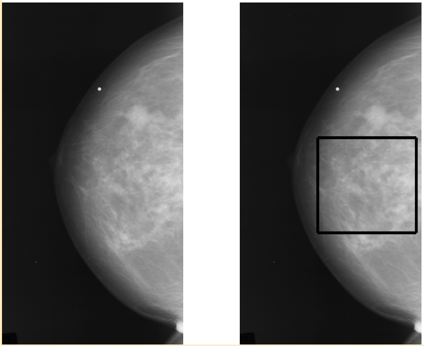

Classification

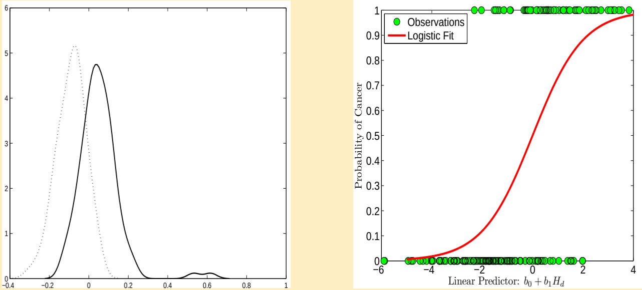

Figure: (Left) Estimated density of H obtained from 105 controls (*solid line*) and 72 cancer cases (*dotted line*); (Right) Logistic fit

Classification

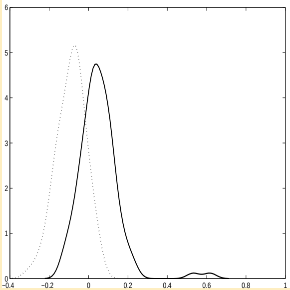

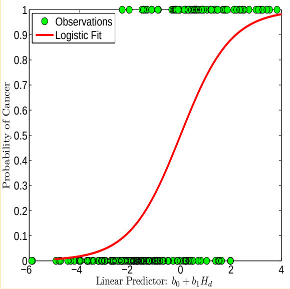

Figure: (Left) Estimated density of H obtained from 105 controls (*solid line*) and 72 cancer cases (*dotted line*); (Right) Logistic fit

- Symmlet 8 tap, $5 \leq j \leq 8$, Found H_{-1}, H, H_{+1} corresponding to $s = 0, \pm 1$.

Classification

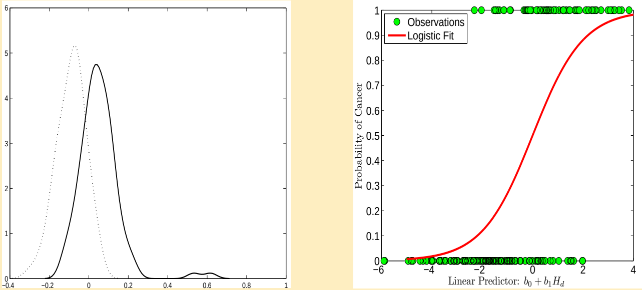

Figure: (Left) Estimated density of H obtained from 105 controls (*solid line*) and 72 cancer cases (*dotted line*); (Right) Logistic fit

- Symmlet 8 tap, $5 \leq j \leq 8$, Found H_{-1}, H, H_{+1} corresponding to $s = 0, \pm 1$.
- 120 randomly selected as training, 57 as validation set

Classification

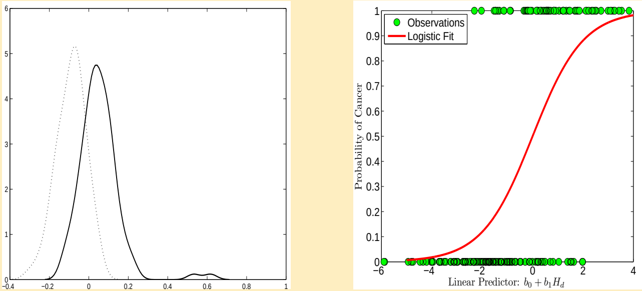

Figure: (Left) Estimated density of H obtained from 105 controls (*solid line*) and 72 cancer cases (*dotted line*); (Right) Logistic fit

- Symmlet 8 tap, $5 \leq j \leq 8$, Found H_{-1}, H, H_{+1} corresponding to $s = 0, \pm 1$.
- 120 randomly selected as training, 57 as validation set
- The most informative was diagonal H, adding descriptors H_{-1}, H_{+1} improves classification, but minimally.

Simulations

Average error rate from $M = 5000$ runs

Method	**Error [%]**
OLS	39.9
Abry-Veitch	24.1
Theil-Sen	25.4
Modified Theil-Sen*	18.2

Simulations

Average error rate from $M = 5000$ runs

Method	**Error [%]**
OLS	39.9
Abry-Veitch	24.1
Theil-Sen	25.4
Modified Theil-Sen*	18.2

Simulations

Average error rate from $M = 5000$ runs

Method	**Error [%]**
OLS	39.9
Abry-Veitch	24.1
Theil-Sen	25.4
Modified Theil-Sen*	18.2

Simulations

Average error rate from $M = 5000$ runs

Method	**Error [%]**
OLS	39.9
Abry-Veitch	24.1
Theil-Sen	25.4
Modified Theil-Sen*	18.2

Simulations

Average error rate from $M = 5000$ runs

Method	**Error [%]**
OLS	39.9
Abry-Veitch	24.1
Theil-Sen	25.4
Modified Theil-Sen*	18.2

*Modified Theil-Sen has weights $\propto\ 2^{i+j}(j-i)^2 HA(2^{2i}, 2^{2j})$

Some Observations

Some Observations

- Sampling density of $Y = \log_2 \overline{d_j^2}$ for fixed H, j, m, and σ^2 is

$$g(y) = \frac{\log 2}{\Gamma(2^{mj-1})} \left(\frac{2^{y+2(H+m)j-1}}{\sigma^2} \right)^{2^{mj-1}} \exp\left\{ -\frac{2^{y+2(H+m)j-1}}{\sigma^2} \right\}$$

Some Observations

- Sampling density of $Y = \log_2 \overline{d_j^2}$ for fixed H, j, m, and σ^2 is

$$g(y) = \frac{\log 2}{\Gamma(2^{mj-1})} \left(\frac{2^{y+2(H+m)j-1}}{\sigma^2} \right)^{2^{mj-1}} \exp\left\{ -\frac{2^{y+2(H+m)j-1}}{\sigma^2} \right\}$$

- Possible distribution of pairwise slopes, Bayesian approach with prior on H, or more generally on (H, σ^2).

Some Observations

- Sampling density of $Y = \log_2 \overline{d_j^2}$ for fixed H, j, m, and σ^2 is

$$g(y) = \frac{\log 2}{\Gamma(2^{mj-1})} \left(\frac{2^{y+2(H+m)j-1}}{\sigma^2} \right)^{2^{mj-1}} \exp\left\{ -\frac{2^{y+2(H+m)j-1}}{\sigma^2} \right\}$$

- Possible distribution of pairwise slopes, Bayesian approach with prior on H, or more generally on (H, σ^2).
- Since $2^{2H(j-i)} \frac{d_{j\bullet}^2}{d_{i\bullet}^2} \sim F_{n_j, n_i}$, for $d_{j\bullet}^2 = \sum_{\boldsymbol{k} \in \text{level } j} d_{j\boldsymbol{k}}^2$ and n_j is the number of d's in level j, $(1-\alpha)100\%$ CI for H is

$$\left[\frac{\log_2 \left(F_{n_j, n_i, \alpha/2} \times \frac{d_{i\bullet}^2}{d_{j\bullet}^2} \right)}{2(j-i)}, \quad \frac{\log_2 \left(F_{n_j, n_i, 1-\alpha/2} \times \frac{d_{i\bullet}^2}{d_{j\bullet}^2} \right)}{2(j-i)} \right]$$

Multifractal Spectra

- Given α,

$$\begin{aligned} f(\alpha) &= \lim_{\epsilon \to 0} \lim_{j \to \infty} \frac{\log_2 M_j}{j} \\ M_j &= \#\{k |\ 2^{-j(\alpha+\epsilon)} \leq |d_{jk}| \leq 2^{-j(\alpha-\epsilon)}\ \}/2^j. \end{aligned}$$

- Partition function:

$$S(q) = \lim_{j \to \infty} \log_2 \mathbb{E}|d_{j,k}|^q.$$

The Legendre transform of a partition function $S(q)$ is defined as

$$f_L(\alpha) = \inf_q \{q\alpha - S(q)\}.$$

- $f_L(\alpha)$ converges to the true multifractal spectrum $f(\alpha)$ (Ellis, 1984).

Multifractal Spectra

Multifractal Spectra

- Gonçalvès, Reidi, and Baraniuk (1998) "Asilomar Paper" discussed discrete wavelet transform Legendre spectra as an approximation to multifractal spectra.

Multifractal Spectra

- Gonçalvès, Reidi, and Baraniuk (1998) "Asilomar Paper" discussed discrete wavelet transform Legendre spectra as an approximation to multifractal spectra.
- In the discrete wavelet transform the "energies" are generalized, $d_{jk}^2 \Longrightarrow |d_{jk}|^q, \; q > -1.$

Multifractal Spectra

- Gonçalvès, Reidi, and Baraniuk (1998) "Asilomar Paper" discussed discrete wavelet transform Legendre spectra as an approximation to multifractal spectra.
- In the discrete wavelet transform the "energies" are generalized, $d_{jk}^2 \Longrightarrow |d_{jk}|^q, \ q > -1.$
- Slope (*partition function*) $S(q)$ found on pairs $(j, \log_2 \overline{|d_j|^q})$

Multifractal Spectra

- Gonçalvès, Reidi, and Baraniuk (1998) "Asilomar Paper" discussed discrete wavelet transform Legendre spectra as an approximation to multifractal spectra.
- In the discrete wavelet transform the "energies" are generalized, $d_{jk}^2 \Longrightarrow |d_{jk}|^q,\ q > -1$.
- Slope (*partition function*) $S(q)$ found on pairs $(j, \log_2 \overline{|d_j|^q})$
- Define Legendre spectra as (α, f) with $\alpha(q) = S'(q)$ and $f(q) = q\alpha(q) - S(q)$.

Multifractal Spectra

- Gonçalvès, Reidi, and Baraniuk (1998) "Asilomar Paper" discussed discrete wavelet transform Legendre spectra as an approximation to multifractal spectra.
- In the discrete wavelet transform the "energies" are generalized, $d_{jk}^2 \Longrightarrow |d_{jk}|^q,\ q > -1$.
- Slope (*partition function*) $S(q)$ found on pairs $(j, \log_2 \overline{|d_j|^q})$
- Define Legendre spectra as (α, f) with $\alpha(q) = S'(q)$ and $f(q) = q\alpha(q) - S(q)$.

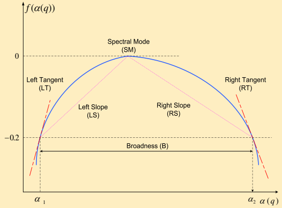

Summaries:
Spectral Mode $\equiv H$
Left Slope, Right Slope
Left Tangent, Right Tangent
Broadness
α_L *and* α_R

• Theil-Sen-type estimator for slopes $S(q), q > -1$ uses the same weights as $S(2)$.

• The variance of $\left(\log_2 \overline{|d_j|^q} - \log_2 \overline{|d_i|^q}\right)/(j-i)$ does depend on q but via a multiplicative factor free of j.

• Theil-Sen-type estimator for slopes $S(q), q > -1$ uses the same weights as $S(2)$.

• The variance of $\left(\log_2 \overline{|d_j|^q} - \log_2 \overline{|d_i|^q}\right)/(j-i)$ does depend on q but via a multiplicative factor free of j.

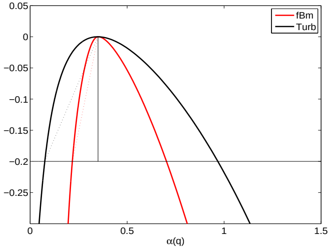

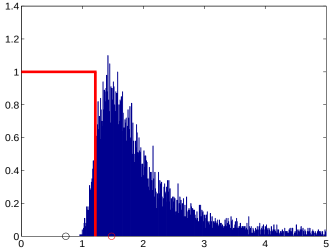

Signal	SM	LS	RS	LT	RT	B
Turb	0.3382	0.7331	-0.3229	2.7500	-0.5400	0.8922
fBm	0.3422	1.4845	-0.5704	3.7400	-0.8700	0.4853

■ Signals with $LS < 1.2144$ significantly different from monofractals.

■ $LS = 1.4845$, $5\% = 1.2144$, $LS = 0.7331$

Wavelet Convex Rearrangements

Let $X(t),\ t \geq 0$ be Gaussian process satisfying $\mathcal{A}$ and let $\boldsymbol{g}$ be a wavelet high-pass filter (QM counterpart of $\boldsymbol{h}$)

Wavelet Convex Rearrangements

Let $X(t),\ t \geq 0$ be Gaussian process satisfying $\mathcal{A}$ and let $\boldsymbol{g}$ be a wavelet high-pass filter (QM counterpart of $\boldsymbol{h}$)
Define $\boldsymbol{g}$-*convex rearrangement* of $X(t)$ as

$$\mathcal{V}X_{\boldsymbol{g},N}(t) = X(0) + \sum_{i=0}^{\lfloor Nt \rfloor - 1} Y_{\boldsymbol{g},(i:N)} + (Nt - \lfloor Nt \rfloor) Y_{\boldsymbol{g},(\lfloor Nt \rfloor : N)},$$

where $\{Y_{\boldsymbol{g},(0:N)}, \ldots, Y_{\boldsymbol{g},(N-1:N)}\}$ is order statistics for the sequence $Y_{\boldsymbol{g}}\left(\frac{k}{N}\right) = \sum_{n=0}^{\ell} g_n X\left(\frac{k-n}{N}\right)$, for $k = 0, 1, \ldots, N-1$.

Wavelet Convex Rearrangements

Let $X(t),\ t \geq 0$ be Gaussian process satisfying $\mathcal{A}$ and let $\boldsymbol{g}$ be a wavelet high-pass filter (QM counterpart of $\boldsymbol{h}$)
Define $\boldsymbol{g}$-*convex rearrangement* of $X(t)$ as

$$\mathcal{V}X_{\boldsymbol{g},N}(t) = X(0) + \sum_{i=0}^{\lfloor Nt \rfloor - 1} Y_{\boldsymbol{g},(i:N)} + (Nt - \lfloor Nt \rfloor) Y_{\boldsymbol{g},(\lfloor Nt \rfloor : N)},$$

where $\{Y_{\boldsymbol{g},(0:N)}, \ldots, Y_{\boldsymbol{g},(N-1:N)}\}$ is order statistics for the sequence $Y_{\boldsymbol{g}}\left(\frac{k}{N}\right) = \sum_{n=0}^{\ell} g_n X\left(\frac{k-n}{N}\right)$, for $k = 0, 1, \ldots, N-1$.
Let $\boldsymbol{g}^d$ be dilation of filter $\boldsymbol{g}$ obtained by inserting $d-1$ zeros between non-zero filter taps. For example, for
$\boldsymbol{g} = \boldsymbol{g}^1 = \{1/\sqrt{2} \quad -1/\sqrt{2}\}$ the 3-dilated filter is
$\boldsymbol{g}^3 = \{1/\sqrt{2} \;\; 0 \;\; 0 \quad -1/\sqrt{2}\}$.

Theorem

Let

$$\mathbb{D}(N, d_1, d_2, t_0) = \frac{\mathcal{V}X_{\boldsymbol{g}^{d_2},N}(t_0)}{\mathcal{V}X_{\boldsymbol{g}^{d_1},N}(t_0)}.$$

Then for any $t_0 \in [0,1]$, and integers d_1, and d_2,

$$\frac{\log|\mathbb{D}(N, d_1, d_2, t_0)|}{\log(d_2/d_1)} \longrightarrow H,\ \ a.s.$$

Idea of proof:
$\frac{\mathcal{V}X_{\boldsymbol{g},N}(t)}{b_N(\boldsymbol{g})} \to L(t) = \int_0^t \Phi^{-1}(s)ds = -\frac{1}{\sqrt{2\pi}} \exp\left\{-\frac{1}{2}\left(\Phi^{-1}(t)\right)^2\right\},\ \ a.s.$
and $\frac{b_N(\boldsymbol{g}^s)}{b_N(\boldsymbol{g}^t)} = (s/t)^H$.

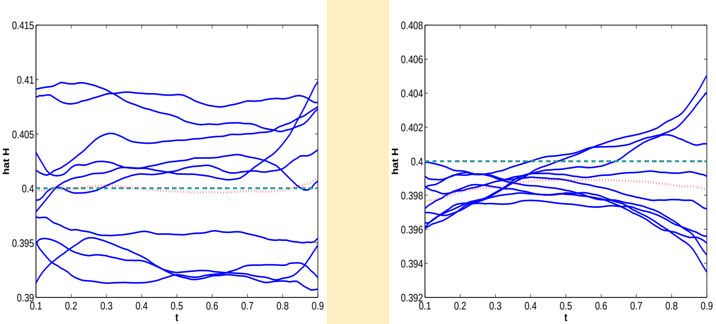

Figure: (Left) 10 runs, $n = 1024$, $d_1 = 1$ and $d_2 = 6$. Symmlet 8 tap filter used. (Right) Single run but Daubechies 4-20 tap filters used

Thanks to collaborators

Thanks to collaborators

- Pepa Ramírez Cobo (Postdoctoral Visitor, U. Seville) Scaling using traditional multidimensional WT; Multifractal spectra summaries; Theil-Sen-type estimators in multifractal spectra; Bayesian approaches; Scale-mixing transforms.

Thanks to collaborators

- Pepa Ramírez Cobo (Postdoctoral Visitor, U. Seville) Scaling using traditional multidimensional WT; Multifractal spectra summaries; Theil-Sen-type estimators in multifractal spectra; Bayesian approaches; Scale-mixing transforms.
- Orietta Nicolis (Postdoctoral Visitor, U. Bergamo) Scaling using traditional multidimensional WT; Complex wavelets.

Thanks to collaborators

- Pepa Ramírez Cobo (Postdoctoral Visitor, U. Seville) Scaling using traditional multidimensional WT; Multifractal spectra summaries; Theil-Sen-type estimators in multifractal spectra; Bayesian approaches; Scale-mixing transforms.
- Orietta Nicolis (Postdoctoral Visitor, U. Bergamo) Scaling using traditional multidimensional WT; Complex wavelets.
- Kichun Sky Lee (Graduated in 2011) Bootstrap tests for monofractality. Estimation of the variance in fBm's.

Thanks to collaborators

- Pepa Ramírez Cobo (Postdoctoral Visitor, U. Seville) Scaling using traditional multidimensional WT; Multifractal spectra summaries; Theil-Sen-type estimators in multifractal spectra; Bayesian approaches; Scale-mixing transforms.
- Orietta Nicolis (Postdoctoral Visitor, U. Bergamo) Scaling using traditional multidimensional WT; Complex wavelets.
- Kichun Sky Lee (Graduated in 2011) Bootstrap tests for monofractality. Estimation of the variance in fBm's.
- Seonghye Jeon (Graduated in 2012) Scaling assessed with complex wavelets

Thanks to collaborators

- Pepa Ramírez Cobo (Postdoctoral Visitor, U. Seville) Scaling using traditional multidimensional WT; Multifractal spectra summaries; Theil-Sen-type estimators in multifractal spectra; Bayesian approaches; Scale-mixing transforms.
- Orietta Nicolis (Postdoctoral Visitor, U. Bergamo) Scaling using traditional multidimensional WT; Complex wavelets.
- Kichun Sky Lee (Graduated in 2011) Bootstrap tests for monofractality. Estimation of the variance in fBm's.
- Seonghye Jeon (Graduated in 2012) Scaling assessed with complex wavelets
- Hinkyeol Woo (Graduated in 2012) Applications of scaling in mass-spectrometry. Multifractal indices as inputs to linear models and data mining tools.

Thanks to collaborators

- Pepa Ramírez Cobo (Postdoctoral Visitor, U. Seville) Scaling using traditional multidimensional WT; Multifractal spectra summaries; Theil-Sen-type estimators in multifractal spectra; Bayesian approaches; Scale-mixing transforms.
- Orietta Nicolis (Postdoctoral Visitor, U. Bergamo) Scaling using traditional multidimensional WT; Complex wavelets.
- Kichun Sky Lee (Graduated in 2011) Bootstrap tests for monofractality. Estimation of the variance in fBm's.
- Seonghye Jeon (Graduated in 2012) Scaling assessed with complex wavelets
- Hinkyeol Woo (Graduated in 2012) Applications of scaling in mass-spectrometry. Multifractal indices as inputs to linear models and data mining tools.
- Erin Hamilton (Ph.D. defense in 2013) Theil-Sen-type estimators of scaling.

Conclusions

- A case for the importance od scaling assessment made
- Spectra from scale-mixing 2D wavelet transform
- An overview of a robust estimator of scaling presented
- Illustration on mammogram medical diagnostics